

Article type : Articles

Running head: Extreme events and alternative states

Title: Temporal clustering of extreme climate events drives a regime shift in rocky intertidal biofilms

Martina Dal Bello^{1,2}, Luca Rindi¹, Lisandro Benedetti-Cecchi¹

¹Department of Biology, University of Pisa, CoNISMa, Via Derna 1, Pisa, Italy

² *Present address:* Physics of Living Systems Group, Department of Physics, Massachusetts Institute of Technology, Cambridge, MA 02139

Correspondence to:

Martina Dal Bello

Tel. +1 617 715 4326

Fax +1 617 258 6883

dalbello@mit.edu

Type of the article: Article ABSTRACT

Research on regime shifts has focused primarily on how changes in the intensity and duration of press disturbances precipitate natural systems into undesirable, alternative states. By contrast, the role of recurrent pulse perturbations, such as extreme climatic events, has been largely neglected, hindering our understanding of how historical processes regulate the onset of a regime shift. We

This is the author manuscript accepted for publication and has undergone full peer review but has not been through the copyediting, typesetting, pagination and proofreading process, which may lead to differences between this version and the [Version of Record](#). Please cite this article as [doi: 10.1002/ECY.2578](https://doi.org/10.1002/ECY.2578)

This article is protected by copyright. All rights reserved

performed field manipulations to evaluate whether combinations of extreme events of temperature and sediment deposition that differed in their degree of temporal clustering generated alternative states in rocky intertidal epilithic microphytobenthos (biofilms) on rocky shores. The likelihood of biofilms to shift from a vegetated to a bare state depended on the degree of temporal clustering of events, with biofilm biomass showing both states under a regime of non-clustered (60 days apart) perturbations while collapsing in the clustered (15 days apart) scenario. Our results indicate that time since the last perturbation can be an important predictor of collapse in systems exhibiting alternative states and that consideration of historical effects in studies of regime shifts may largely improve our understanding of ecosystem dynamics under climate change.

Keywords: alternative states, extreme events, regime shift, epilithic microphytobenthos, biofilm, climate change, temporal clustering, abrupt changes

INTRODUCTION

Ecosystems often display non-linear responses to both gradual and abrupt changes in driving variables (e.g. temperature, nutrient loading), undergoing catastrophic transitions known as regime shifts (Scheffer et al. 2001, Scheffer and Carpenter 2003). Most theoretical and experimental work on regime shifts has focused on gradual changes in the intensity of a press disturbance (the driver variable), showing that many ecosystems can absorb such changes and maintain their current state up to a threshold beyond which they transition to an alternative, less desirable state (Petraitis and Dudgeon 2004, Dakos et al. 2008, Scheffer et al. 2012, Benedetti-Cecchi et al. 2015, Rindi et al. 2017). Only recently, ecologists have recognized the importance of temporal characteristics of press disturbances in regulating regime shifts. Ratajczak et al. (2017) showed that the duration of the perturbation is crucial for the onset of regime shifts in systems that respond slowly to external change and that exhibit strong coupling between past and present dynamics. In contrast, our understanding of the role of recurrent pulse events and how the history of previous perturbations affects the susceptibility of ecosystems to undergo a regime shift is still limited.

Pulse events such as fires, the outbreak of natural enemies and extreme climatic events have a great potential to induce regime shifts (Scheffer et al. 2001). In highly stochastic environments, species coexistence is promoted by the capacity of species to respond differentially to environmental fluctuations. Each population, then, is able to store the gains coming from good periods and use them to survive losses in bad periods, a phenomenon known as storage effect, which ultimately allows a community to maintain biodiversity (Chesson 2000). Pulse perturbations, however, may exceed tolerance limits of organisms, causing impairment of function or outright mortality of individuals (Schröder et al. 2005). If also resting stages are affected, pulse events may prevent species coexistence by disrupting storage effects. Pulse disturbances can also influence community dynamics and biodiversity by selectively removing community dominants, thereby freeing up resources for other species and reducing community's biotic resistance to invasive species (Walker et al. 2005, Mumby et al. 2011). Any of these changes may translate into a system being suddenly pushed beyond the unstable region separating the basins of attraction of the contrasting states, resulting in a regime shift (Scheffer et al. 2001).

The likelihood of a pulse perturbation to push a system into an alternative state depends upon its location with respect to the critical threshold; the more the system is close to the threshold, the higher is the likelihood of a transition (Folke et al. 2004, van der Bolt et al. 2018). Moreover, ecosystems are exposed to multiple, recurrent perturbations, so that the likelihood of a regime shift may also depend on the particular regime of disturbance the system has experienced (Paine et al. 1998). Specifically, the characteristics of a regime of pulse disturbances that may leave strong historical signatures on ecosystem dynamics include the nature, the order and the timing of occurrence of perturbations (Benedetti-Cecchi et al. 2015, Dantas et al. 2016, Dal Bello et al. 2017). Although alterations of disturbance scenarios are already receiving a great amount of attention in the ecological literature, how variation in the regime of pulse perturbations affect regime shifts has been largely neglected.

Extreme climatic events are becoming more common and severe as a consequence of climate change (Fischer and Knutti 2015) and they can induce abrupt transitions in terrestrial and aquatic ecosystems (Holmgren et al. 2006, Wernberg et al. 2016). There is general consensus that the effects of extreme events vary with their nature and temporal regimes (Benedetti-Cecchi et al. 2006, Mumby et al. 2011, Williams et al. 2011). Moreover, recent studies showed that

changes in the temporal clustering of extreme events, i.e. the degree of separation between consecutive instances, can modulate ecological memory of microbial assemblages (Dal Bello et al. 2017) and regulate the onset of regime shifts in tropical ecosystems (Holmgren et al. 2013). Evaluating how different scenarios of extreme events can trigger a regime shift in systems with alternative states will be a crucial step to better understand the impact of climate change on ecosystems.

Here, we address this challenge using rocky intertidal epilithic microphytobenthos (biofilms) as model system. We focused on extreme events of temperature and sediment deposition after heavy rains, since these are major drivers of biofilm abundance and distribution (Thompson et al. 2004, Dal Bello et al. 2017). We used photosynthetic biofilms primarily because it is a tractable system for field experiments, being the result of the activity of fast growing organisms, which display rapid responses to perturbations (Christofoletti et al. 2011). Moreover, we expected alternative states in biofilms due to stabilizing mechanisms that operate both at high and low values of biomass. High biomass values sustain high photosynthesis rates, which, in turn, support enhanced production of extracellular polymeric substances (EPS) (Wulff et al. 2000, Wolfstein and Stal 2002). EPS, being the major components of the dense matrix in which microalgal cells are embedded, provide protection against stressful conditions, e.g. heat stress during low tides and further boost photosynthesis and biomass accumulation (Flemming and Wingender 2010). This positive feedback can be eroded by processes that either remove biomass or degrade EPS, e.g. high temperatures, abrasion due to sediment scouring, wave action (Decho 2000, Thompson et al. 2004). We propose that such losses trigger runaway changes propelling the switch from a “vegetated” to a “bare” (or “semi-bare”) state. The semi-bare state will be then maintained due to the uncoupling of photosynthesis and EPS production at low biofilm biomass values (“*Allee effect*”). Such feedback can work both ways: the more the biomass, the higher the growth and the less the biomass, the lower the growth. Positive feedback loops like this one may be responsible for the catastrophic effect of extreme events, similarly to what observed in microcosm experiments with yeasts populations, which show cooperative growth and a negative growth rate at low cells density (Dai et al. 2012).

We used a field experiment and a model to test for the presence of alternative states in rocky shore photosynthetic biofilms and to explore the underlying feedback mechanisms. The field experiment tested the hypothesis that series of extreme events of temperature and sediment

deposition that differed in their degree of temporal clustering induced alternative states in biofilm assemblages. Multimodality in the frequency distribution of biofilm biomass (Scheffer et al. 2012, Sirota et al. 2013) and divergence in the temporal trajectories of experimental units belonging to the same treatment (Scheffer and Carpenter 2003, Schröder et al. 2005) are both indirect indications for the presence of alternative states, here a vegetated and a semi-bare state (Schröder 2009). Based on the results of a previous study (Dal Bello et al. 2017), we anticipate that the vegetated state would correspond to the biomass in the controls, while the semi-bare state would reflect reduced biofilm biomass in the clustered perturbation scenario. This is expected because extreme events clustered in time may push the system below a threshold biomass value, impairing the ability of biofilm to recover to the vegetated state. Moreover, we expect two modes in the non-clustered scenario, where two perturbations separated in time may be able to push some experimental units in the semi-bare state, while others, due to small initial differences in biomass, may remain in the vegetated state. To further explore the effects of temporal clustering of extreme events on biofilm biomass, we parametrized a simple model that incorporated the positive feedback between photosynthesis and EPS production through an “Allee effect”.

MATERIALS AND METHODS

Study area

The experiment was done along the coast of Calafuria (Livorno, 43°30' N, 10°19' E) between April and August 2013. The coast consists of gently sloping sandstone platforms with high-shore levels (0.3 - 0.5 m above mean low-level water) colonized by assemblages of barnacles interspersed among areas of seemingly bare rock, where photosynthetic biofilms develop. Biofilm assemblages at Calafuria include mainly cyanobacteria, with diatoms being less abundant (Maggi et al. 2017). The most important grazer at this height on the shore is the littorinid snail *Melaraphe neritoides* (L). During the experiment, however, grazing pressure over biofilm assemblages was nearly absent (Dal Bello et al. 2017).

Experimental design

Along Mediterranean rocky shores, highly thermally stressing periods of calm sea and high barometric pressure alternate with heavy rainfalls, the latter resulting in the deposition of sediments at tidal heights where photosynthetic biofilms develop (Airoldi 2003, Benedetti-

Cecchi et al. 2006, Dal Bello et al. 2017). In order to mimic this pattern, we imposed different series of extreme events of warming and sediment deposition. A scenario characterized by non-clustered events was created by imposing two extreme disturbances 60 days apart, while two disturbances 15 days apart characterized the clustered condition. The non-clustered scenario was conceived to allow biofilm biomass to recover between the two events, whilst recovery was considered unlikely in the time window separating clustered events. Since biofilm is composed of fast-growing species with short generation time, an interval of 60 days was sufficiently long to allow recovery and therefore the two perturbations could be considered as separate events. For each level of clustering, we imposed all the possible combinations of warming and sediment deposition: two consecutive sediment deposition events, two consecutive extreme warming events, one extreme sediment deposition event followed by an extreme warming episode, an extreme warming event followed by an extreme sediment deposition episode. Extreme warming was obtained by artificially increasing air temperature over experimental plots using aluminum chambers equipped with stoves. The treatment consisted in maintaining the air temperature inside the chambers as close as possible to 32 °C during the two hours corresponding to the peak in daily temperatures, i.e. around midday in all instances. The temperature chosen represents the 100-years return time temperature for the months in which the experiment was performed (Katz et al. 2005). Procedural controls for artifacts (CA) were set-up to control for the effects of shading on biofilm biomass due to the use of non-transparent heating chambers. CA plots were therefore kept in shaded conditions but without heating for the duration of the warming treatment by means of cardboard chambers. Sediment addition on experimental plots was used to simulate the effects of runoff after a heavy rainfall event. The treatment consisted in adding a 5mm-thick layer of sediment collected *in situ* and diluted in fresh water to produce the colloidal material that is naturally deposited on rocky shores after severe precipitation events. Three experimental plots were assigned to each combination of extreme events of disturbance. Three unmanipulated plots were used as controls (C) and six plots were used as procedure controls of artefacts (CA). Experimental plots were located 2-10 meters apart and consisted of areas of substratum of 30 x 50 cm marked at their corners with raw-plugs inserted into the rock for subsequent relocation.

Data collection and analyses

Biofilm biomass was quantified indirectly by means of an image-based remote sensing technique that uses chlorophyll *a* concentration as a proxy. Chlorophyll *a* was estimated from the ratio of

reflectance at near-infrared (NIR) and red bands (Ratio Vegetational Index - RVI) obtained by means of an IR-sensitive camera, following the method proposed by Murphy et al. (2006). NIR/red ratios are linked to the chlorophyll content in the rock by a linear relationship, calculated on the basis of laboratory chlorophyll *a* extractions from Calafuria sandstone cores (Dal Bello et al. 2015).

Experimental plots were monitored in time after the imposition of both experimental perturbations, with the non-clustered scenario sampled at days 70, 84, 108, 133 and the clustered scenario sampled at days 81, 91, 109, 138, counting from day 0 (i.e. when the experiment started and we imposed the first extreme of the non-clustered scenario) (see Appendix 1: Fig. S1). Controls were sampled also at days 5, 20 and 55, in addition to days 70, 84, 91, 108 and 133 (Appendix 1: Fig. S1). Once in the lab, each image was handled with a routine in ImageJ software to haphazardly select 5 subplots of 256 x 256 pixels and to provide a mean estimate of biofilm biomass for each of them.

The presence of alternative states was tested indirectly through the evaluation of multimodality in the frequency distribution of biofilm biomass (Scheffer et al. 2012, Sirota et al. 2013). The number of modes in the frequency distribution of biofilm biomass values was estimated at the first sampling date after the second perturbation event for both non-clustered and clustered scenario (days 70 and 81 from the start of the experiment, respectively), while we used data from the four dates after the second perturbation event to assess divergence among temporal trajectories of biofilm biomass. The number of modes has been identified with normal mixture modelling and model-based clustering using Mclust package in R. We used bootstrapping to calculate 95% confidence intervals. For each level of temporal clustering (control, clustered and non-clustered), observations were resampled 999 times and modes were estimated. 95% confidence intervals were calculated as 2.5th and 97.5th percentile of the vector of bootstrapped modes (Davison et al. 1997).

Another qualitative indicator for the presence of alternative states is the divergence of temporal trajectories of identically treated experimental units (Scheffer and Carpenter 2003). In particular, alternative state theory predicts that the final state of a system, vegetated or semi-bare in our case, will depend on the initial position of the state variable with respect to a threshold: units with biofilm biomass above the threshold at the first sampling date will remain in the vegetated state, while units below that threshold will shift to the semi-bare state (Schröder et al.

2005). To test this, we adopted a binary classification technique commonly used in machine learning: given the value of biofilm biomass at the first sampling date after both extreme events, the algorithm decides whether that particular unit will end up in the semi-bare (0) or in the vegetated state (1). In this case the algorithm was a binomial generalized linear model that we fit to our data using the *glm* function in the R package stats (version 3. .5.1). We divided the data belonging to the non-clustered scenario into two groups: 1) a training set, consisting of 60% of data points, in which an experimental unit was classified as vegetated if its biomass was embraced in the confidence interval of the mean control biomass at the last sampling date or semi-bare otherwise, and 2) a testing set including the remaining 40% of the data. The training set was used to fit the binomial generalized linear model, whose accuracy was then tested over the testing set.

Model formulation and parameterization

We developed a simple mathematical model to explore whether different temporal regimes of temperature extremes could induce alternative states in biofilm biomass. We considered only one stressor variable since extremes warming and sediment deposition events have comparable effects on biofilm biomass (Dal Bello et al. 2017). The goal here was to assess biofilm dynamics under different temporal scenarios of temperature extremes and to test whether the degree of temporal clustering could generate alternative states. This model provided a qualitative benchmark with which to compare the experimental results.

We modelled the dynamics of biofilm using a simple growth equation describing changes of biofilm biomass ($\mu\text{g chl } a \text{ cm}^{-2}$) as a function of temperature and a loss equation, which reflects general processes leading to biofilm mortality (e.g. consumption by grazers and dislodgment by waves):

$$\frac{dB}{dt} = G(B) - F(B) + \sigma B \frac{dT}{dt} \quad (\text{Eq. 1})$$

where B is the biomass of biofilm ($\mu\text{g chl } a \text{ cm}^{-2}$), t is time and T is mean air temperature ($^{\circ}\text{C}$). Function $G(B)$ is a logistic equation that describes the growth of biofilm biomass, in which the per capita growth rate varies as a function of mean air temperature ($^{\circ}\text{C}$). Function $F(B)$ describes the loss of biomass due to biological or physical disturbance. Due to the narrow amplitude of tides, intertidal organisms along Mediterranean coasts may be exposed to elevated desiccation

stress due to prolonged periods of calm seas and high barometric pressure. In contrast, waves and rough sea conditions can keep intertidal organisms constantly wet, even during low tides (Benedetti-Cecchi et al. 2006). Frequent shocks to biofilm biomass due to such contrasting and rapidly changing weather conditions are represented in the model by the term $\sigma B dW/dt$, where dW/dt is a Wiener white noise process with mean 0 and variance dt and σ is the scale parameter of the noise process, which was arbitrarily set to 0.04.

As anticipated before, the $G(B)$ function is a logistic equation describing the growth of biofilm biomass:

$$G(B) = r(T)B \left(1 - \frac{B}{K}\right) \quad (\text{Eq. 2})$$

where $r(T)$ is a two-phase thermal performance curve modelling the variation of growth rate as a function of temperature and K is maximum biofilm biomass (Deutsch et al. 2008, Vasseur et al. 2014) (Appendix S1: Fig. S2).

$$r(T) = \begin{cases} r_{\max} \left[1 - \frac{(T - T_{\text{opt}})}{T_{\text{opt}} - T_{\max}}\right]^2 & T \geq T_{\text{opt}} \\ r_{\max} \left[e^{\left[\frac{(T - T_{\text{opt}})^2}{2\sigma_p}\right]}\right] & T < T_{\text{opt}} \end{cases} \quad (\text{Eq. 3})$$

where r_m is the maximum growth rate of biofilm biomass, T is air temperature, T_{opt} is the mean air temperature at which the growth rate is maximum ($r(T_{\text{opt}}) = r_{\max}$), T_{\max} is the temperature limit beyond which the growth rate becomes negative, and σ_p is a parameter controlling the rate of increase of growth rate in the ascending part of the curve. This relationship is in line with experimental evidence and observations that higher values of air temperature (T °C) strongly decreased the growth rate of rocky intertidal biofilms (Sanz-Lázaro et al. 2015, Dal Bello et al. 2017).

The model included an “*Allee effect*” implying a lower growth rate at low levels of biomass. We assumed that the mortality rate of biofilm increased below a certain value of biomass, due to the decrease in EPS production and the consequent increase in desiccation stress and reduction of protection against UV radiation (Potts 1999, Wulff et al. 2000, Wolfstein and Stal 2002):

$$F(B) = m_a B \left(\frac{h_A}{B + h_A}\right) \quad (\text{Eq. 4})$$

The loss term caused a net reduction of per capita growth rate at low biomass levels. This was achieved through a Monod equation with a half-saturation constant h_a , which defines the biomass level below which this loss term is halved.

Model parametrization and simulations

Parameters were estimated empirically by fitting the model to time series of biofilm biomass at the study site (Appendix S1: Table 1). On nine occasions between April and August 2013 we sampled six plots the same size as the experimental units (30 x 50 cm) and biofilm biomass was evaluated as described in the previous section. Daily temperature data were obtained from Rete Mareografica Nazionale (ISPRA, <http://www.mareografico.it>). Maximum likelihood parameter estimates were obtained with the *mle2* function of the *bmle* library in R, assuming lognormal errors (Bolker 2008). Predicted time series were obtained by integrating over time initial biofilm biomass. We used the *ode* function of R package *deSolve*, with backward differentiation formula (Soetaert et al. 2012). We used plot averages of biofilm biomass for this analysis because subplots within plots differed among dates, so only data aggregated at the plot level could be tracked through time (Appendix S1: Fig. S2). The interpolating function *aproxfun* in the R package *deSolve* was used to obtain temperature estimates at exact time points during the integration routine. Likelihood profiles were inspected to ensure that parameters were well defined.

To evaluate the effect of extreme climatic events in the model, we first generated a baseline condition where air temperature increased from 23 to 27.5 °C, which resembled the increase in temperature observed during the experiment (data obtained by from Rete Mareografica Nazionale, ISPRA, <http://www.mareografico.it>). Moreover, to reproduce the variability in mean temperature similar to that observed over the study period, we superimposed to temperature time series a white noise process with mean (μ) zero and standard deviation (σ) equal to 1.5 °C. Time series of air temperature were finally modified to integrate the maximum air temperature measured in the experimental warming session (aerial temperature of 32 °C). As in the experiment, we produced two temporal patterns of extreme events, a clustered pattern in which we imparted two warming events separated by 15 days (day 76 and day 91) and a non-clustered scenario consisting of the same temperature extreme separated by 60 days (day 10 and day 70; Appendix S1: Fig. S1). We constructed a set of simulated time series for each scenario running Eq. 1 from 50 different initial conditions randomly selected from a normal distribution

($\mu = 3.5$, $\sigma = 0.5$), for 150 time-steps. Also, a third set of simulations without the imposition of extreme events was produced. Simulations were performed by using an Euler-Murayama method with Ito calculus (Iacus 2009).

RESULTS

Biofilm biomass exhibited two distinct states (Fig. 1). Biomass distribution in controls (no extreme events) was unimodal and centered on the value of $4.59 \mu\text{g chl } a \text{ cm}^{-2}$ (95% CIs [4.23 - 4.97]), which identifies the vegetated state (Fig. 1A, D, see Table 1). The distribution of biomass in the clustered scenario was also unimodal but centered on a lower value ($1.23 \mu\text{g chl } a \text{ cm}^{-2}$; 95% CIs [1.08 - 1.38]), which identifies a semi-bare state (Fig. 1B, D and Table 1). Non-clustered event treatments showed instead bimodality ($1.61 \mu\text{g chl } a \text{ cm}^{-2}$; 95% CIs [1.25 - 1.91] and $4.38 \mu\text{g chl } a \text{ cm}^{-2}$; 95% CIs [3.63 - 4.89]), with intermediate values of biofilm biomass (Fig. 1C, D and Table 1). Graphical scrutiny of the results suggests that warming and sediment deposition have similar effects on the distribution of biofilm biomass (Appendix S1: Fig. S3).

Inspection of the temporal trajectories of biofilm biomass revealed that, despite a slight decline, controls remained in the vegetated state during the course of the study, while clustered treatments were consistently in the semi-bare state. The non-clustered scenario showed a divergent pattern, with some experimental units recovering to biomass values observed in controls and other units declining towards values measured in the clustered treatments (Fig. 2). In the non-clustered scenario, whether a unit recovered to the vegetated state or declined to the semi-bare state depended on its value of biomass at the first sampling date (Appendix S1: Fig S4). In particular, a unit increase in biofilm biomass increased the probability (log odds) to end up in the bare state by 1.88 (Table 2). Finally, the model predicted the final state of experimental units in the testing set with reasonable accuracy (AUC=0.9, Appendix S1: Fig. S5).

The response of biofilm biomass to extreme events in the model was consistent with the experimental results (Fig. 3). In the non-clustered scenario, time series of biofilm biomass showed a marked divergent pattern, with some replicates recovering and others collapsing. This resulted in a bimodal frequency distribution, with one mode of $\sim 0 \mu\text{g chl } a \text{ cm}^{-2}$ and the other of $\sim 3 \mu\text{g chl } a \text{ cm}^{-2}$ (Fig. 3a). In the clustered scenario, instead, biofilm biomass collapsed, showing a unimodal pattern with a mode corresponding to $\sim 0 \mu\text{g chl } a \text{ cm}^{-2}$ (Fig. 3b). In the controls, biofilm biomass showed a slight decrease over time and a unimodal pattern in the frequency

distribution, with a mode of $\sim 3 \mu\text{g chl } a \text{ cm}^{-2}$ (Fig. 3c). Although the model clearly produced a bimodal pattern, the frequencies distribution in the experiment did not exactly match the pattern produced by the simulation, with the experimentally observed modes slightly greater than the ones predicted by the model.

DISCUSSION

Our findings suggest that the history of extreme events and the time since the last perturbation may affect the susceptibility of rocky intertidal photosynthetic biofilms to undergo a regime shift. The analysis of the frequency distribution of biofilm biomass indicated the occurrence of two alternative states under a regime of non-clustered extremes: a semi-bare state characterized by low biomass and a vegetated state where biomass was high, separated by an unstable range of biomass values. In contrast, clustered extremes induced the collapse of biofilm biomass precipitating the system in the semi-bare state.

Assessing multimodality in the frequency distribution of state variables has been often used as a qualitative flag to assess the consistency between empirical data and theoretical expectations of catastrophic transitions (Scheffer et al. 2012). Assessing whether a system shows alternative states also involves testing for the temporal random divergence of identically treated experimental units (Schröder et al. 2005). This implies that, in a bistable system strongly influenced by stochastic perturbations, some experimental units will tend to one state and others will converge towards the other state and the outcome depends on initial conditions. Yet, observing a state transition and lack of recovery following the application of pulse perturbations provides a stringent test for alternative states in natural systems (test for non-recovery, Suding et al. 2004, Schröder et al. 2005). Biofilm biomass in the clustered scenario exhibited a state transition toward the semi-bare state and a complete lack of recovery which persisted for two months following the imposition of extreme events. Our experimental results together with model simulations were consistent with these expectations, showing how experimental units with intermediated values of biomass followed divergent trajectories, culminating to either the semi-bare or the vegetated state in the non-clustered scenario.

Self-replacement, the capacity of an assemblage to maintain itself over time, is a proxy for stability of alternative states (Connell and Sousa 1983). Biofilm at our study site was mainly composed of cyanobacteria characterised by fast-growing species with short generation time (from days to weeks) (Whitton 2012, Maggi et al. 2017). The persistence of the two alternative

states for a time encompassing several generations of the species composing biofilm (two months in our study) suggests that the two alternative states may be considered stable *sensu* Connell and Sousa (1983). On the contrary, in our study we did not investigate whether alternative states were locally stable, for instance, whether the semi-bare state recovered to a vegetated state upon the arrival of new individuals from the water column (Beisner et al. 2003). One approach would involve the application of a small perturbation (e.g. a small clearing) at each of the two contrasting states to test whether or not they returned to the original condition. Previous studies have shown that biofilm may experience drastic changes in biomass and recover from apparently catastrophic transitions within a relatively short time scale (Alsterberg et al. 2007, Larson and Sundbäck 2012). Although we cannot entirely rule out that vegetated and the semi-bare state represent alternative transient states (*sensu* Fukami and Nakajima 2011), our results support the hypothesis that biofilm may shift from a vegetated to a semi-bare state in response to multiple pulses of temperature and sediment deposition.

Our results are important in light of the predicted increase in the frequency of extreme climatic events under climate change (IPCC 2013). The degree of temporal clustering of extremes is expected to increase, as signalled by increased variance in the interval of time between events in tropical ecosystems (Mumby et al. 2011, Holmgren et al. 2013), grasslands (Fuchslueger et al. 2016) and Mediterranean coastal areas (Volosciuk et al. 2016). Changes in temporal clustering can moderate the severity of ecological impacts caused by extreme events (Benedetti-Cecchi et al. 2006, Holmgren et al. 2006, Kreyling et al. 2011, Mumby et al. 2011) and modulate the ecological memory of natural systems (Dal Bello et al. 2017). Here we highlight that the degree of temporal clustering of extremes may regulate the occurrence of regime shifts.

Exogenous periodic forces and seasonality may affect the ability of a natural system to respond to extreme events and, in general, to stochastic pulse perturbations. Our study shows that biofilm biomass decreased along the course of the experiment, from spring to summer. A similar decline in biofilm biomass has been described in other studies and likely reflects the effect of increasing temperature and light intensity (Nagarkar and Williams 1999, Jackson et al. 2010). Biofilm assemblages likely experienced progressively stressful conditions during the course of the experiment, which made them more susceptible to collapse as summer proceeded. As temperature increased during the experiment, the capacity of biofilm to recover from a

temperature extreme drastically decreased, making it more susceptible to a subsequent perturbation. In agreement with these experimental results, the biofilm model indicated that seasonal warming amplified the impact of temporally clustered perturbations. When sudden perturbations occur in combination with unfavourable environmental conditions (e.g. higher summer temperatures), their compounded effects may have dramatic consequences. Such contingencies may, thus, play a pivotal role in determining the occurrence of tipping points and alternative states in natural systems.

Thermal buffering provided by conspecifics is a widespread facilitative mechanism in rocky intertidal communities (Stachowicz 2001). Biofilms should benefit from living at high density due to higher EPS production, which in turn enhances survival and boosts growth (Potts 1994, Steele et al. 2014). Our experimental results showed how extreme temperatures may push biofilm biomass toward a threshold level, below which growth rates can no longer compensate for increased mortality. As shown in another study, EPS production decreases with declining growth rates of biofilm, hence increasing the risk of lethal damages due to enhanced thermal stress when a critical level of low biofilm biomass is reached (Wulff et al. 2000). At this point the production of EPS becomes too low and it is no longer effective in protecting biofilm from stressful conditions. This mechanism generates feedbacks, so that the resulting loss of biomass further weakens the facilitative effect of EPS. Our experimental and model results support the view that the combined effect of greater mortality at low biomass (“*Allee effect*”), a mechanism that may reflect the reduction of EPS production, along with seasonal changes in aerial temperature markedly affect biofilm biomass temporal dynamics.

Biofilm assemblages consist of microscopic photosynthetic organisms and, despite their small size they strongly contribute to the primary productivity of intertidal rocky shores (Thompson et al. 2004). A wealth of studies showed that changes in primary productivity affect higher trophic levels (Wernberg et al. 2016, Guo et al. 2017, but see Liess et al. 2015 for a counter example). Since fast growing microbial populations are an important component of primary producers in virtually all ecosystems, increasing temporal clustering of extreme events will likely have pervasive impacts on food webs, altering biological interactions and affecting the stability of whole ecosystems. Our results should therefore prompt new studies investigating the cascading effects of regime shifts in primary producer communities.

Current research on regime shifts has mainly focused on investigating how gradual changes in ecological drivers precipitate natural systems into undesirable, alternative states. Only recently, ecological research turned its attention to the examination of the effects of other types of disturbances, such as recurrent pulse events. Here, we show that ecosystem dynamics can be largely affected by extreme events, with the likelihood of a regime shift primarily depending on the time separating consecutive events. However, further work is needed to determine the generality of these results to better understand and predict ecosystem dynamics in a rapidly changing world.

ACKNOWLEDGMENTS

We thank A. Schröder and an anonymous reviewer for their constructive comments to the manuscript. We also thank Elena Maggi, Chiara Ravaglioli and several students for assistance with the field work. This research was supported by the University of Pisa through the PRA programme (PRA_2017_19) and the Italian Ministry of Research and Education through the PRIN grant ‘Biocostruzioni costiere: struttura, funzione e gestione’ to LBC. The first and second authors contributed equally to this work.

REFERENCES

- Airoidi, L. 2003. The effects of sedimentation on rocky coast assemblages. *Oceanography and marine biology: an annual review* **41**:161-236.
- Alsterberg, C., K. Sundbäck, and F. Larson. 2007. Direct and indirect effects of an antifouling biocide on benthic microalgae and meiofauna. *Journal of Experimental Marine Biology and Ecology* **351**:56-72.
- Benedetti-Cecchi, L., I. Bertocci, S. Vaselli, and E. Maggi. 2006. Temporal Variance Reverses the Impact of High Mean Intensity of Stress in Climate Change Experiments. *Ecology* **87**:2489-2499.

- Benedetti-Cecchi, L., L. Tamburello, E. Maggi, and F. Bulleri. 2015. Experimental Perturbations Modify the Performance of Early Warning Indicators of Regime Shift. *Current Biology* **25**:1867-1872.
- Bolker, B. M. 2008. *Ecological Models and Data* in R. Princeton University Press.
- Chesson, P. 2000. Mechanisms of Maintenance of Species Diversity. *Annual Review of Ecology and Systematics* **31**:343-366.
- Christofoletti, R. A., T. V. V. Almeida, and Á. Ciotti. 2011. Environmental and grazing influence on spatial variability of intertidal biofilm on subtropical rocky shores. *Marine Ecology Progress Series* **424**:15-23.
- Dai, L., D. Vorsele, K. S. Korolev, and J. Gore. 2012. Generic indicators for loss of resilience before a tipping point leading to population collapse. *Science* **336**:1175-1177.
- Dakos, V., M. Scheffer, E. H. van Nes, V. Brovkin, V. Petoukhov, and H. Held. 2008. Slowing down as an early warning signal for abrupt climate change. *Proceedings of the National Academy of Sciences, USA* **105**:14308-14312.
- Dal Bello, M., E. Maggi, L. Rindi, A. Capocchi, D. Fontanini, C. Sanz-Lazaro, and L. Benedetti-Cecchi. 2015. Multifractal spatial distribution of epilithic microphytobenthos on a Mediterranean rocky shore. *Oikos* **124**:477-485.
- Dal Bello, M., L. Rindi, and L. Benedetti-Cecchi. 2017. Legacy effects and memory loss: how contingencies moderate the response of rocky intertidal biofilms to present and past extreme events. *Glob Chang Biol.* **23**:3259-3268

- 470 Dantas, V. d. L., M. Hirota, R. S. Oliveira, and J. G. Pausas. 2016. Disturbance maintains
471 alternative biome states. *Ecol Lett* **19**:12-19.
- 472 Davison, A. C., D. V. Hinkley, and A. J. Canty. 1997. *Bootstrap Methods and Their Application*.
473 Cambridge University Press.
- 474 Decho, A. W. 2000. Microbial biofilms in intertidal systems: an overview. *Continental Shelf*
475 *Research* **20**:1257-1273.
- 476 Deutsch, C. A., J. J. Tewksbury, R. B. Huey, K. S. Sheldon, C. K. Ghalambor, D. C. Haak, and
477 P. R. Martin. 2008. Impacts of climate warming on terrestrial ectotherms across latitude.
478 *Proc Natl Acad Sci U S A* **105**:6668-6672.
- 479 Fischer, E. M., and R. Knutti. 2015. Anthropogenic contribution to global occurrence of heavy-
480 precipitation and high-temperature extremes. *Nature Climate Change* **5**:560-564.
- 481 Flemming, H. C., and J. Wingender. 2010. The biofilm matrix. *Nature Reviews: Microbiology*
482 **8**:623-633.
- 483 Folke, C., S. Carpenter, B. Walker, M. Scheffer, T. Elmqvist, L. Gunderson, and C. S. Holling.
484 2004. Regime Shifts, Resilience, and Biodiversity in Ecosystem Management. *Annual*
485 *Review of Ecology, Evolution, and Systematics* **35**:557-581.
- 486 Fuchslueger, L., M. Bahn, R. Hasibeder, S. Kienzl, K. Fritz, M. Schmitt, M. Watzka, and A.
487 Richter. 2016. Drought history affects grassland plant and microbial carbon turnover
488 during and after a subsequent drought event. *Journal of Ecology* **104**:1453-1465.
- 489 Fukami, T., and M. Nakajima. 2011. Community assembly: alternative stable states or alternative
490 transient states? *Ecology Letters* **14**:973-984.

491 Guo, H., C. Weaver, S. P. Charles, A. Whitt, S. Dastidar, P. D'Odorico, J. D. Fuentes, J. S.
 492 Kominoski, A. R. Armitage, and S. C. Pennings. 2017. Coastal regime shifts: rapid
 493 responses of coastal wetlands to changes in mangrove cover. *Ecology* **98**:762-772.

494 Holmgren, M., M. Hirota, E. H. van Nes, and M. Scheffer. 2013. Effects of interannual climate
 495 variability on tropical tree cover. *Nature Climate Change* **3**:755-758.

496 Holmgren, M., P. Stapp, C. R. Dickman, C. Gracia, S. Graham, J. R. Gutiérrez, C. Hice, F.
 497 Jaksic, D. A. Kelt, M. Letnic, M. Lima, B. C. López, P. L. Meserve, W. B. Milstead, G.
 498 A. Polis, M. A. Previtalli, M. Richter, S. Sabaté, and F. A. Squeo. 2006. Extreme climatic
 499 events shape arid and semiarid ecosystems. *Frontiers in Ecology and the Environment*
 500 **4**:87-95.

501 Iacus, S. M. 2009. *Simulation and Inference for Stochastic Differential Equations: With R*
 502 *Examples*. Springer New York.

503 IPCC. 2013. Annex I: Atlas of Global and Regional Climate Projections Pages 1311–1394 in T.
 504 F. Stocker, D. Qin, G.-K. Plattner, M. Tignor, S. K. Allen, J. Boschung, A. Nauels, Y.
 505 Xia, V. Bex, and P. M. Midgley, editors. *Climate Change 2013: The Physical Science*
 506 *Basis. Contribution of Working Group I to the Fifth Assessment Report of the*
 507 *Intergovernmental Panel on Climate Change*. Cambridge University Press, Cambridge,
 508 United Kingdom and New York, NY, USA.

509 Jackson, A. C., A. J. Underwood, R. J. Murphy, and G. A. Skilleter. 2010. Latitudinal and
 510 environmental patterns in abundance and composition of epilithic microphytobenthos.
 511 *Marine Ecology Progress Series* **417**:27-38.

512 Katz, R. W., G. S. Brush, and M. B. Parlange. 2005. Statistics of Extremes: Modeling Ecological
 513 Disturbances. *Ecology* **86**:1124-1134.

- 514 Kreyling, J., G. Jurasinski, K. Grant, V. Retzer, A. Jentsch, and C. Beierkuhnlein. 2011. Winter
515 warming pulses affect the development of planted temperate grassland and dwarf-shrub
516 heath communities. *Plant Ecology & Diversity* **4**:13-21.
- 517 Larson, F., and K. Sundbäck. 2012. Recovery of microphytobenthos and benthic functions after
518 sediment deposition. *Marine Ecology Progress Series* **446**:31-44.
- 519 Liess, A., O. Rowe, S. N. Francoeur, J. Guo, K. Lange, A. Schröder, B. Reichstein, R. Lefebure,
520 A. Deininger, P. Mathisen, and C. L. Faithfull. 2015. Terrestrial runoff boosts
521 phytoplankton in a Mediterranean coastal lagoon, but these effects do not propagate to
522 higher trophic levels. *Hydrobiologia* **766**:275-291.
- 523 Maggi, E., L. Rindi, M. Dal Bello, D. Fontanini, A. Capocchi, L. Bongiorni, and L. Benedetti-
524 Cecchi. 2017. Spatio-temporal variability in Mediterranean rocky shore
525 microphytobenthos. *Marine Ecology Progress Series* **575**:17-29.
- 526 Mumby, P. J., R. Vitolo, and D. B. Stephenson. 2011. Temporal clustering of tropical cyclones
527 and its ecosystem impacts. *Proc Natl Acad Sci U S A* **108**:17626-17630.
- 528 Murphy, R. J., A. J. Underwood, and M. H. Pinkerton. 2006. Quantitative imaging to measure
529 photosynthetic biomass on an intertidal rock-platform. *Marine Ecology Progress Series*
530 **312**:45-55.
- 531 Nagarkar, S., and G. A. Williams. 1999. Spatial and temporal variation of cyanobacteria-
532 dominated epilithic communities on a tropical shore in Hong Kong. *Phycologia* **38**:385-
533 393.
- 534 Paine, R. T., M. J. Tegner, and E. A. Johnson. 1998. Compounded Perturbations Yield
535 Ecological Surprises. *Ecosystems* **1**:535-545.

- 536 Petraitis, P. S., and S. R. Dudgeon. 2004. Detection of alternative stable states in marine
537 communities. *Journal of Experimental Marine Biology and Ecology* **300**:343-371.
- 538 Potts, M. 1994. Desiccation tolerance of prokaryotes. *Microbiological Reviews* **58**:755-805.
- 539 Potts, M. 1999. Mechanisms of desiccation tolerance in cyanobacteria. *European Journal of*
540 *Phycology* **34**:319-328.
- 541 Ratajczak, Z., P. D'Odorico, S. L. Collins, B. T. Bestelmeyer, F. I. Isbell, and J. B. Nippert.
542 2017. The interactive effects of press/pulse intensity and duration on regime shifts at
543 multiple scales. *Ecological Monographs* **87**:198-218.
- 544 Rindi, L., M. D. Bello, L. Dai, J. Gore, and L. Benedetti-Cecchi. 2017. Direct observation of
545 increasing recovery length before collapse of a marine benthic ecosystem. *Nature*
546 *Ecology & Evolution* **1**:0153.
- 547 Sanz-Lázaro, C., L. Rindi, E. Maggi, M. Dal Bello, and L. Benedetti-Cecchi. 2015. Effects of
548 grazer diversity on marine microphytobenthic biofilm: a 'tug of war' between
549 complementarity and competition. *Marine Ecology Progress Series* **540**:145-155.
- 550 Scheffer, M., S. Carpenter, J. A. Foley, C. Folke, and B. Walker. 2001. Catastrophic shifts in
551 ecosystems. *Nature* **413**:591-596.
- 552 Scheffer, M., and S. R. Carpenter. 2003. Catastrophic regime shifts in ecosystems: linking theory
553 to observation. *Trends in Ecology & Evolution* **18**:648-656.
- 554 Scheffer, M., M. Hirota, M. Holmgren, E. H. Van Nes, and F. S. Chapin, 3rd. 2012. Thresholds
555 for boreal biome transitions. *Proc Natl Acad Sci U S A* **109**:21384-21389.

- 556 Schröder, A. 2009. Inference about complex ecosystem dynamics in ecological research and
557 restoration practice. Pages 50-62 in H. R. J. and S. K. N., editors. New models for
558 ecosystem dynamics and restoration. Washington, Island Press.
- 559 Schröder, A., L. Persson, and A. M. De Roos. 2005. Direct experimental evidence for alternative
560 stable states: a review. *Oikos* **110**:3-19.
- 561 Sirota, J., B. Baiser, N. J. Gotelli, and A. M. Ellison. 2013. Organic-matter loading determines
562 regime shifts and alternative states in an aquatic ecosystem. *Proc Natl Acad Sci U S A*
563 **110**:7742-7747.
- 564 Soetaert, K., J. Cash, and F. Mazzia. 2012. Solving Differential Equations in R. Springer Berlin
565 Heidelberg.
- 566 Stachowicz, J. J. 2001. Mutualism, Facilitation, and the Structure of Ecological Communities.
567 *Bioscience* **51**:235.
- 568 Steele, D. J., D. J. Franklin, and G. J. Underwood. 2014. Protection of cells from salinity stress
569 by extracellular polymeric substances in diatom biofilms. *Biofouling* **30**:987-998.
- 570 Suding, K. N., K. L. Gross, and G. R. Houseman. 2004. Alternative states and positive feedbacks
571 in restoration ecology. *Trends in Ecology & Evolution* **19**:46-53.
- 572 Thompson, R. C., T. A. Norton, and S. J. Hawkins. 2004. Physical Stress and Biological Control
573 Regulate the Producer–Consumer Balance in Intertidal Biofilms. *Ecology* **85**:1372-1382.
- 574 van der Bolt, B., E. H. van Nes, S. Bathiany, M. E. Vollebregt, and M. Scheffer. 2018. Climate
575 reddening increases the chance of critical transitions. *Nature Climate Change* **8**:478-484.

576 Vasseur, D. A., J. P. DeLong, B. Gilbert, H. S. Greig, C. D. Harley, K. S. McCann, V. Savage, T.
 577 D. Tunney, and M. I. O'Connor. 2014. Increased temperature variation poses a greater
 578 risk to species than climate warming. *Proc Biol Sci* **281**:20132612.

579 Volosciuk, C., D. Maraun, V. A. Semenov, N. Tilinina, S. K. Gulev, and M. Latif. 2016. Rising
 580 Mediterranean Sea Surface Temperatures Amplify Extreme Summer Precipitation in
 581 Central Europe. *Sci Rep* **6**:32450.

582 Walker, S., J. Bastow Wilson, and W. G. Lee. 2005. Does fluctuating resource availability
 583 increase invasibility? Evidence from field experiments in New Zealand short tussock
 584 grassland. *Biological Invasions* **7**:195-211.

585 Wernberg, T., S. Bennett, R. C. Babcock, T. de Bettignies, K. Cure, M. Depczynski, F. Dufois, J.
 586 Fromont, C. J. Fulton, R. K. Hovey, E. S. Harvey, T. H. Holmes, G. A. Kendrick, B.
 587 Radford, J. Santana-Garcon, B. J. Saunders, D. A. Smale, M. S. Thomsen, C. A. Tuckett,
 588 F. Tuya, M. A. Vanderklift, and S. Wilson. 2016. Climate-driven regime shift of a
 589 temperate marine ecosystem. *Science* **353**:169-172.

590 Williams, G. A., M. De Pirro, S. Cartwright, K. Khangura, W. C. Ng, P. T. Y. Leung, and D.
 591 Morritt. 2011. Come rain or shine: the combined effects of physical stresses on
 592 physiological and protein-level responses of an intertidal limpet in the monsoonal tropics.
 593 *Functional Ecology* **25**:101-110.

594 Wolfstein, K., and L. J. Stal. 2002. Production of extracellular polymeric substances (EPS) by
 595 benthic diatoms: effect of irradiance and temperature. *Marine Ecology Progress Series*
 596 **236**:13-22.

597 Wulff, A., S.-Å. k. Wängberg, K. Sundbäck, C. Nilsson, and G. J. C. Underwood. 2000. Effects
 598 of UVB radiation on a marine microphytobenthic community growing on a sand-

substratum under different nutrient conditions. Limnology and Oceanography **45**:1144-1152.

Table 1. BIC criterion of models with a different number of fitted density distributions (here we show the first 4) for control, non-clustered and clustered scenarios. The model with the smallest BIC (in bold) has the best fit.

<i>Modes</i>	Controls (no extremes)	Non-clustered events	Clustered events
1	223.9490	238.5700	118.1841
2	231.3705	231.1430	120.7077
3	241.5501	243.4187	‡
4	251.3868	249.2830	‡

‡ No convergence

Table 2. Binomial generalized linear model on the final state of experimental units (semi-bare or vegetated state) as a function of the value of biofilm biomass at the first sampling date after both extreme events. An experimental unit is assigned to the vegetated state if its biomass value is embraced in the 95% confidence interval of the mean control biomass at the last sampling date; otherwise it is classified as semi-bare state. McFadden R^2 indicates the goodness of fit.

* $p < 0.05$, ** $p < 0.01$, *** $p < 0.001$

	Coefficient (SE)	
Intercept	-8.46 (3.19)	**
Biomass at the first sampling date	1.88 (0.71)	**

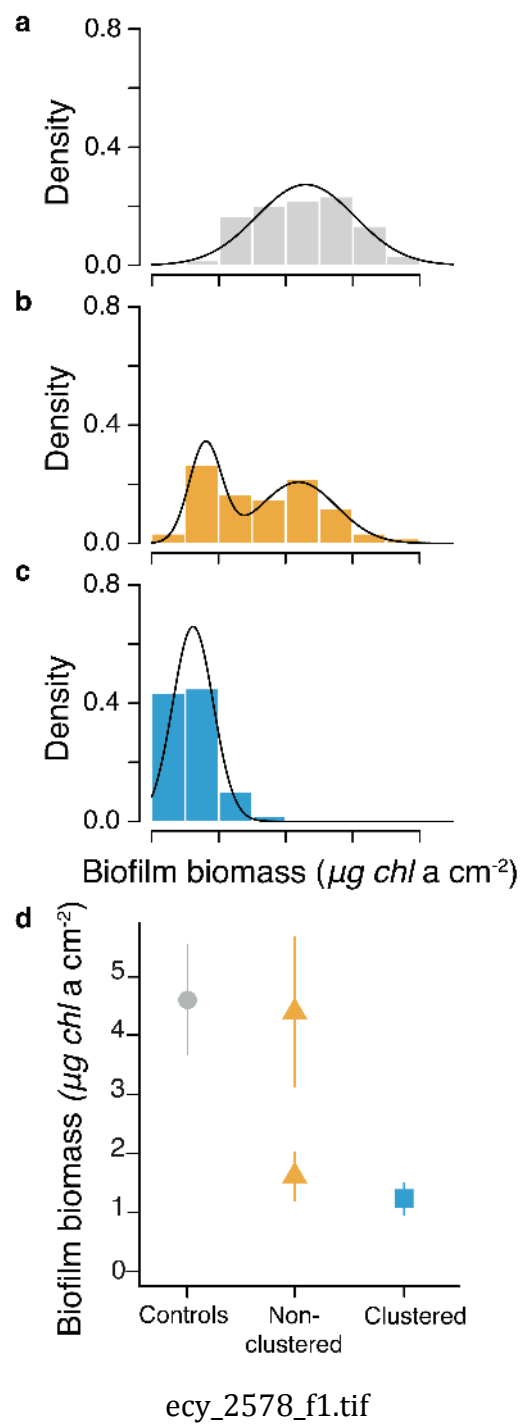
McFadden $R^2 = 52\%$

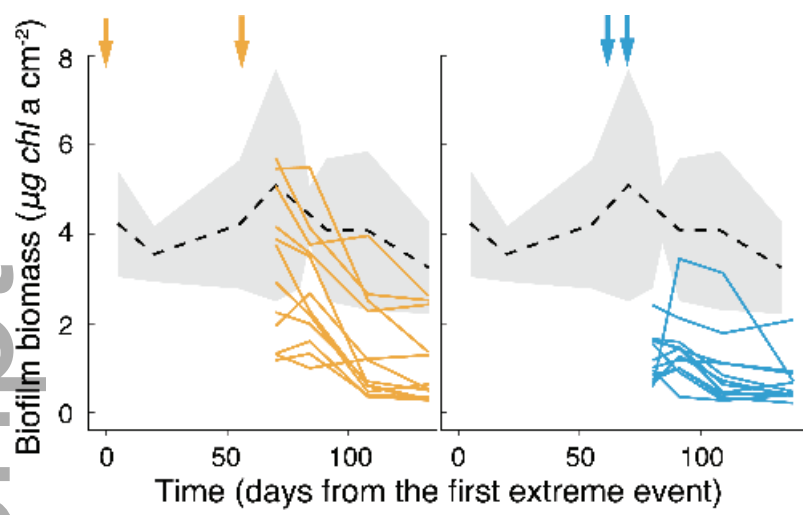
LEGEND TO FIGURES

Figure 1. Frequency distribution of biofilm biomass and probability density functions (solid lines) separately for controls (panel a), non-clustered (panel b) and clustered events treatments (panel c). In panel d, the modes for each experimental condition are shown together with bootstrapped 95% confidence intervals.

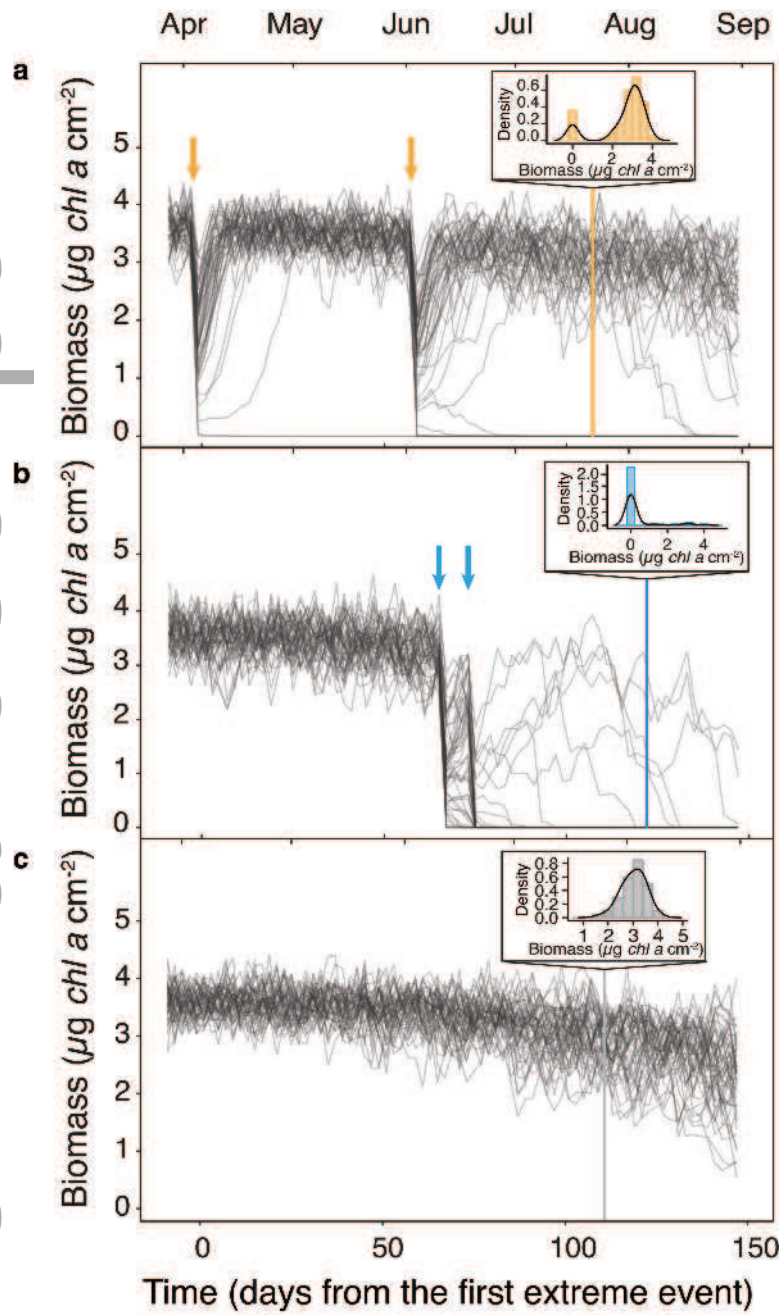
Figure 2. Observed temporal trajectories of biofilm biomass under the non-clustered (left panel) and the clustered (right panel) scenarios of extreme climatic events, indicated as days from the first experimental perturbation. The control treatment is used for reference and is shown as 95% confidence interval region (light grey) and averaged temporal trajectory (black). Arrows indicate the timing of the perturbations for non-clustered (orange) and clustered (blue) events.

Figure 3. Simulated temporal trajectories of biofilm biomass ($\mu\text{g chl } a \text{ cm}^{-2}$) for (a) non-clustered and (b) clustered warming regimes. In panel (c) there are controls. Time series were computed from simulations with 50 replicates over a time span of 160 days for increasing mean air temperature from 22 to 27 °C. Warming in the simulation mirrored the observed increase in temperature during the study period (data obtained from Rete Mareografica Nazionale ISPRA, <http://www.mareografico.it>). Down-facing arrows indicate the timing of perturbations. We simulated two temporal patterns of ECEs: a clustered pattern in which we imparted two warming events (aerial temperature of 32 °C) separated by 15 days, and a non-clustered scenario consisting of the same temperature extremes separated by 60 days. The initial periods of 10 days were excluded from the visualization to remove transient dynamics. The insets show the frequency distributions and probability density functions (solid lines) of biofilm biomass under non-clustered and clustered warming regimes calculated for the day indicated by the colored bar.





ecy_2578_f2.tif



ecy_2578_f3.tif